

# Design, characterization and biopharmaceutical behaviour of Nanoparticles loaded with an HIV-1 Fusion Inhibitor Peptide

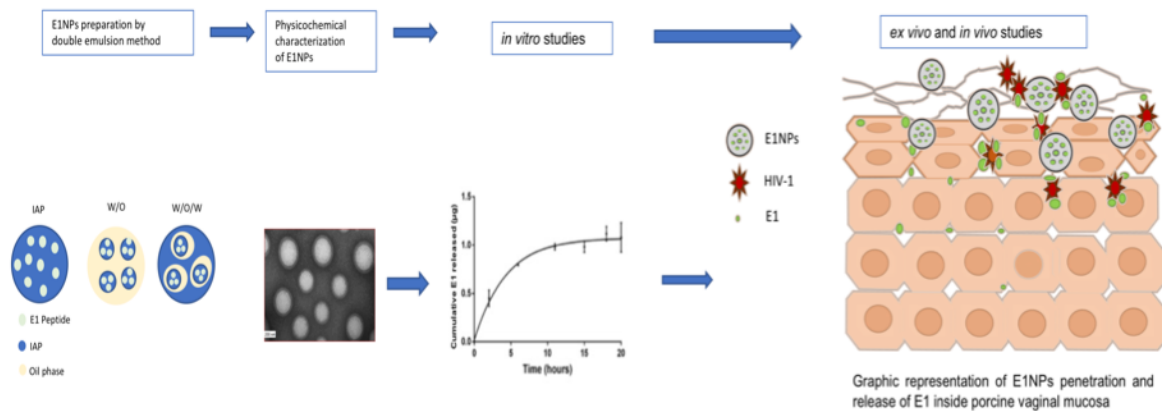
*Martha Ariza-Sáenz<sup>\*1,2</sup>, Marta Espina<sup>1</sup>, Ana Calpena<sup>1</sup>, María J. Gómara<sup>2</sup>, Ignacio Pérez-Pomeda<sup>2</sup>,  
Isabel Haro<sup>2</sup> and María Luisa García<sup>1</sup>*

<sup>1</sup>Department of Pharmacy and Pharmaceutical Technology and Physical Chemistry, University of  
Barcelona, Av. Joan XXIII, 27-31, Barcelona 08028, Spain

<sup>2</sup>Unit of Synthesis and Biomedical Application of Peptides, Department of Biomedical  
Chemistry, IQAC-CSIC, Jordi Girona 18, 08034 Barcelona, Spain

## KEY WORDS

GB virus C, HIV-1; Fusion inhibitor peptide of HIV-1; Polymeric Nanoparticles; Factorial  
Design; Permeation Studies.



## ABSTRACT

New therapeutic alternatives to fight against the spread of HIV-1 are based on peptides designed to inhibit the early steps of HIV-1 fusion in target cells. However, drawbacks such as: bioavailability, short half-life, rapid clearance and poor ability to cross the physiological barriers make such peptides unattractive for the pharmaceutical industry. Here we developed, optimized and characterized polymeric nanoparticles (NPs) coated with glycol chitosan (GC) to incorporate and release an HIV-1 fusion inhibitor peptide (E1), inside the vaginal mucosa. The NPs were prepared by a modified double emulsion method and optimisation was carried out by a factorial design. *In vitro*, *ex vivo* and *in vivo* studies were carried out to evaluate the optimized formulation. The results indicate that the physicochemical features of these NPs enable them to incorporate and release HIV fusion inhibitor peptides to the vaginal mucosa before the fusion step takes place.

## 1. INTRODUCTION

The GB virus C (GBV-C) is a non-pathogenic virus identified and classified as belonging to the flaviviridae family<sup>1</sup>. GBV-C has attracted considerable research attention because it has been associated with a decrease in the morbidity and mortality rate of individuals co-infected with HIV-1. Furthermore, a meta-analysis found that HIV patients with GBV-C viraemia survive longer than those without viraemia<sup>2</sup>. GBV-C is a lymphotropic virus that replicates in human peripheral blood mononuclear cells (PBMCs), including B and T lymphocytes (CD4<sup>+</sup> and CD8<sup>+</sup> subsets)<sup>3</sup>. PBMC co-infection with GBV-C and HIV inhibits HIV replication<sup>4</sup>.

The E1 and E2 envelope proteins of GBV-C are associated with the inhibition HIV-1 replication *in vitro*. These class II fusion proteins are non-helical and have a fusion peptide within internal loop structures, far from the N-terminus<sup>5</sup>. Several studies have described and characterized fragments belonging to GBV-C envelope proteins that may be involved in inhibiting HIV-1 fusion to cells. The inhibition capacity of these peptides has been tested in various biological systems including blood cells, lipids mixtures and Langmuir monolayers<sup>6-8</sup>. These assays have shown that: (a) E2-derived peptides bind to gp4, preventing oligomerisation of the HIV-1 fusion peptide on the membrane, thus inhibiting its destabilisation, which is essential for HIV-1 fusion to the cell membrane; and (b) E1-derived peptides may bind in a highly conserved region on gp41 (fusion peptide) before pre-hairpin formation, which inhibits HIV fusion and entry<sup>9,10</sup>. Some authors have proposed using these peptides to develop new strategies to fight against HIV-1<sup>11-13</sup>, since these inhibitor peptides specifically target the sites where the earlier steps of HIV fusion take place. However, they present shortcomings, such as low oral bioavailability, a short half-life and rapid clearance, which render them unsuitable for the pharmaceutical industry<sup>14</sup>.

The virus is mainly transmitted vaginally and rectally, but the pH and enzymes of the vaginal fluid lining the epithelium present a major obstacle preventing antiretroviral drugs and biomolecules such as peptides from reaching the vaginal epithelium. These drawbacks may be

overcome by using nanoparticle (NP) delivery systems, which entrap large molecules such as proteins and polypeptides and release them to the target tissue without damaging it.

Currently there are over 50 molecules which are candidates to be anti-HIV microbicides and which are in the pre-clinical phases, and another 12 in clinical phases. The most frequently used alternatives for microbicide treatment are the polymer NPs. The NPs manufactured with polymers, such as PLGA, are being investigated, as these devices can overcome the typical problems of drugs such as the biological half-life, conformational stability, physio-chemical stability, solubility and immunological response <sup>15</sup>.

In addition to PLGA, polymers, which act against the transmission of the virus on their own, have been investigated. This is the case of anionic polymers, which stick to the viral envelope and block the entrance of the virus into the target cell. Along these lines, the fabrication of microbicides has been proposed. Their formulation is to be the combination of therapeutic effects, from the transporter material of which they are made, specifically polyanionic materials, and an anti-retroviral drug <sup>16</sup>.

In the light of the facilities that the vaginal mucosa offers for treatment with drugs, several studies have been carried out using NPs to encapsulate and release anti-HIV drugs into the vaginal mucosa<sup>17</sup>. For example, the anti-retroviral drug Tenofovir has been released in a sustained manner from nanofibers with special physio-chemical and surface properties that guarantee the safety and integrity of the mucosa <sup>18</sup>.

Combined therapy based on the development of NPs is another alternative being considered as an important platform in the prevention of HIV. Some authors propose developing an anti-HIV microbicide looking for an approach to different problems such as the maintenance of the biological conditions of the vaginal mucosa, (pH, bacterial flora) as well as how to prevent the viral infection at the same time throughout the invasive stages <sup>19</sup>.

Another aspect that has been studied is the benefits of the NPs in the development of anti-HIV microbicides. This is because these systems offer versatility in the modulation of the drug release: a slow and sustained liberation of the drug is of vital importance to its acceptance <sup>20</sup>

Nanoparticle systems offer several specific advantages over other delivery systems. For instance, they can improve the stability of peptides and maintain their physicochemical properties. They can easily be manipulated to prevent premature release. They may increase the effectiveness and reduce the side effects of the drugs they carry and they can be modified with surface ligands to achieve a specific target <sup>21</sup>. In addition, NPs made with polyesters such as poly (D, L-lactic-co-glycolic acid) (PLGA) offer the further advantages of biocompatibility, biodegradability and non-toxicity <sup>22</sup>. As for PLGA, they have been investigated for their ability to enhance tissue permeability. Leading on from this, it has been described that PLGA nanoparticles do not compromise the cell monolayer integrity<sup>23,24</sup> .

PLGA polymers have been approved by the Food and Drug Administration (FDA) and used as colloidal carriers for controlled drug release, <sup>25</sup> and this is the reason why PLGA NPs have been used as drug carriers for topical administration mixed with polysaccharides such as chitosan <sup>26,27</sup> .

Chitosan is a chitin derivative that enhances permeation through the vaginal mucosa, and it has been widely used in manufacturing of nanoparticles. It has excellent biocompatibility and little toxicity, probably because of its natural origin. Additionally, it prolongs residence time in tissues and has been widely and effectively used in the transport of macromolecules such as peptides and proteins. This is because chitosan adheres to mucus and enhances the efficient permeation of NPs loaded with peptides and proteins <sup>28</sup>. Another advantage described by some authors is that polymeric nanoparticles coated with chitosan substantially increase the bioavailability and efficacy when administered by via vaginal route <sup>29,30</sup> .

Techniques based on double emulsions have been the most commonly used method for the encapsulation of hydrophilic molecules such as peptides and proteins. This method has significant advantages over other techniques such as drying by pulverization (spray drying), and supercritical fluid. For example, the latter method has two principal drawbacks: (a) the poor performance of the powder obtained (low powder yield), and (b) the agglomeration of particles that can lead to the loss of the biological activity of the biomolecule <sup>31</sup>. In the administration route, the drying method has been used for the fabrication of particles when they are intended to

be administered by inhalation. However, the double emulsion method has been successfully used in the fabrication of particles for topical administration and thus has become the most suitable method in the creation of NPs loaded with anti- HIV biomolecules for the vaginal and rectal delivery <sup>32</sup>.

For all the reasons indicated above, and due to the drawbacks of the other methods, we have considered the double emulsion method as the best choice to deliver the anti-HIV synthetic peptide, that has been defined in our group <sup>9</sup>, into the vaginal tissue. The preparation of PLGA-chitosan NPs by means of the double emulsion method for the peptide encapsulation is valid. Glycol-chitosan (GC) coated PLGA-NPs were developed with the capacity to incorporate an HIV-1 inhibitor peptide (E1) and then released into porcine vaginal epithelium. To this end, NP preparation was optimized by a factorial design. Transmission electron microscopy (TEM), X-ray and IR assays were used to analyze morphological and physicochemical properties. *In vitro*, *ex vivo* and *in vivo* assays were performed with optimized and characterized formulations. Interactions between E1NPs and HeLa cells expressing HIV-1 envelope proteins were analyzed by flow cytometry. In addition, *ex vivo* and *in vivo* permeation studies were performed using porcine vaginal mucosa as a animal model.

The novelty of the paper lies in the preparation of a formulation based on a fusion inhibitor peptide that has been previously described by our group, as well as *in vitro*, *ex vivo* and *in vivo* studies, and that it is potentially viable as a microbicide <sup>9</sup>. As has recently been described, antiretroviral-based strategies for HIV prevention have shown inconsistent results in women <sup>33</sup>. Regarding clinical trials on women, the efficacy of vaginal-applied Tenofovir gel to prevent HIV infection ranged from 0% in FACTS trials to 39% in CAPRISA trials. Thus, the study of other formulations based on new fusion inhibitors that impede the entry of the HIV-1 into the host cells could improve the efficacy of antiretroviral drugs when they are jointly applied as microbicides.

## 2. MATERIALS AND METHODS

The chemicals and materials used in this study are described in the *Supplementary Material section*.

### 2.2 Experimental Section

#### 2.2.1. Peptide synthesis

The E1 peptide was synthesised by the Fmoc/tBu strategy of solid-phase peptide synthesis (SPPS) using a NovaSyn® TGR resin (500 mg, 0.25 meq/g). Couplings were achieved by HATU/DIPEA activation with a molar excess of Fmoc-amino acids (3 meq/g). The E1 peptidyl resin was labelled with 5(6)-carboxyfluorescein. E1 and E1-FAM were then purified by a semipreparative high-performance liquid chromatography (HPLC) method. Peptide synthesis is described in more detail in the *Supplementary Material section*.

#### 2.2.2. Preparation of Nanoparticles

The Nanoparticles (NPs) were prepared using a modified double emulsion method<sup>34-36</sup>. Before optimisation, several trial batches were carried out to determine the maximum entrapment efficiency (EE) rate of the peptide and a suitable NP diameter that reached the vaginal epithelium (between 200 and 300 nm). The variables considered for NPs optimization were: (a) the poly(lactic-co-glycolic acid) (PLGA) polymer concentration (mg); (b) polyvinyl alcohol (PVA) concentration (mg); (c) E1 concentration (mg); (d) the inner aqueous phase (IAP) composition and volume; and (e) the pH of the IAP. Resomer® RG 503 H, Poly (D, L-lactide-co-glycolide) (PLGA) was selected as the most appropriate polymer since the NPs made with this polymer incorporated more than 50% of the peptide. NPs with E1 and empty NPs were prepared separately. The preparation and purification of the NPs were carried out following the methodology described in Ariza-Sáenz et al.,<sup>37</sup> with some modifications: 1.5 mg of E1 peptide was solubilized in a mixture of Hepes 50mM (pH 7.2) and acetonitrile (ACN) forming an IAP. Next, 50 mg of PLGA was dissolved in 1 ml of dichloromethane obtaining the organic phase (OP). Briefly, a primary emulsion water-in-oil was formulated by emulsifying the IAP with OP

(50 W, 30 sec). 0.05 % (w/v) of Glycol chitosan (GC) was dissolved in 2.5 % (w/v) polyvinyl alcohol (PVA) acidic solution (pH 4.2) and stirred magnetically. Afterwards, secondary emulsion (water/oil/water) was obtained by adding the primary emulsion drop wise to the PVA solution containing GC, followed by probe sonication (50 W, 60 sec). The resultant emulsion was stirred vigorously over-night to evaporate the organic phase and to obtain the NPs. Once the NPs had been fabricated, the suspension was deposited in a centrifuging tube of polyacrylate and centrifuged at 15000 rpm during 15 min at 4° C and washed twice with Milli-Q water to remove excess PVA-GC and free peptide. Supernatants were storage to determine the free peptide by HPLC UV-VIS validated method (*see supplementary materials section*).

### **2.2.3. Central composite factorial design**

A factorial design was applied to determine the minimum number of experiments required for optimized E1NPs synthesis. A three-factor, five-level central composite rotatable design  $2^3+star$ <sup>38</sup>, was used to evaluate the main effects and interactions of three factors on average particle size (Z-Ave), polydispersity (PI) and EE. The three factors selected, E1 concentration ( $X_1$ ), IAP volume ( $X_2$ ) and polymer concentration (PLGA) in the organic phase ( $X_3$ ), were studied at five different levels coded as  $-\alpha$ ,  $-1$ ,  $0$ ,  $1$  and  $+\alpha$ . The value for alpha (1.682) was calculated to obtain rotatability in the design. The codes and values of the variables are given in *Table S7 in the supplementary materials section*. According to the central composite design matrix generated by the Statgraphics Plus version 5.1 software (Sigma Plus), a total of 16 experiments were required, including 8 factorial points, 6 axial points and 2 replicated center points for estimating the pure error sum of squares (*Table S8 supplementary materials section*). The effects and interactions between the variables or factors were calculated. To determine the effect of a factor  $x$  ( $E_x$ ), the following equation was applied:

$$E_x = \frac{\Sigma x(+)-\Sigma x(-)}{\frac{n}{2}} \quad (1)$$

where  $\Sigma x (+)$  is the sum of the factors at their highest level (+1),  $\Sigma x (-)$  the sum of the factors at their lowest level (-1) and  $n/2$  is half of the number of measurements used in the calculation. The interactions between the factors were also evaluated. To estimate an interaction between two factors, the effect of the first factor at the lowest level of the second one had to be estimated, subtracting it from the effect of the first factor at the highest level of the second one. An interaction between two factors is symbolized as factor 1: factor 2.

The experimental responses studied were the results of the individual influence and the interactions of the three independent variables. The responses were therefore modelled by the following full second-order polynomial equation:

$$Y = \beta_0 + \beta_1 X_1 + \beta_2 X_2 + \beta_3 X_3 + \beta_{11} X_1^2 + \beta_{22} X_2^2 + \beta_{33} X_3^2 + \beta_{12} X_1 X_2 + \beta_{13} X_1 X_3 + \beta_{23} X_2 X_3 \quad (2)$$

where  $Y$  is the measured response,  $\beta_0$  the intercept,  $\beta_1$ ,  $\beta_2$  and  $\beta_3$  the linear coefficients,  $\beta_{11}$ ,  $\beta_{22}$  and  $\beta_{33}$  the squared coefficients,  $\beta_{12}$ ,  $\beta_{13}$  and  $\beta_{23}$  the interaction coefficients, and  $X_1$ ,  $X_2$  and  $X_3$  the independent variables.

Statgraphics Plus version 5.1 (Sigma Plus) was used for the statistical analysis of the data. To determine the significance of the effects and interactions between them, analysis of variance (ANOVA) was performed for each parameter. A  $p$  value less than 0.05 was considered statistically significant.

#### 2.2.4. Physicochemical characterization of NPs

The physicochemical characterization of the NPs was achieved by measuring the Z-Ave and PI. NP surface charge was measured as the zeta potential ( $\zeta$ ) and the EE percentage of the peptide loaded into the NPs was determined indirectly by determining the concentration of the

peptide that was not incorporated into the NPs. In short, after centrifugation of NPs, 50 µl of the supernatant that containing the peptide was injected into HPLC system equipped with a C18 column and an absorbance dual detector (Waters 2487). Mobile phases applied were: ACN /TFA 0.05% and Milli-Q water /TFA 0.05 %. Separation was performed by applying linear gradient from 5 % to 95 % (ACN/TFA 0.05 %) over 20 min at a flow rate of 1 ml/min. Peptide detection was performed by absorbance at 265 nm. Peptide concentration was calculated using the following equation.

$$EE \% = \frac{\text{Total amount of peptide-free peptide}}{\text{total amount of peptide}} \times 100 \quad (3)$$

#### **2.2.5. X-Ray and FTIR studies**

The physical state of the peptide in the NPs and the possible interactions between the peptide and the PLGA were determined by X-ray and Fourier transform infrared (FTIR) spectroscopy. The E1NPs suspension was centrifuged, and the pellet that contained 1.2 mg of peptide was dried under vacuum conditions before being dried to a constant weight in a desiccator.

##### **2.2.5.1. Fourier transform infrared studies**

The FTIR spectra of E1NPs and their compounds (peptide, PLGA and GC) were obtained using a Thermo Scientific Nicolet iZ10 FTIR spectrometer with a diamond attenuated total reflectance (ATR) (DTGS detector; Nichrome source; KBr beamsplitter), with a total of 32 scans (resolution, 4 cm<sup>-1</sup>). The spectra were collected and manipulated using the OMNIC (version. 7.3) software supplied by the manufacturer of the spectrometer. The spectra of each sample were collected in triplicate. The FTIR spectra of E1NPs were obtained using a deuterated-triglycine sulphate (DTGS) detector. The scanning range was 525 – 4000 cm<sup>-1</sup>.

#### **2.2.5.2. X-ray studies**

The X-ray analyses were carried out to evaluate either crystalline or amorphous state of NPs. X-ray powder diffractograms were recorded on a Siemens D500 system (Karlsruher, Germany) using Cu K $\alpha$  radiation (45 kV, 40 mA,  $\lambda = 1.5418 \text{ \AA}$ ). The range scan was ( $2\theta$ ) from  $2^\circ$  to  $60^\circ$  for a step size of  $0.026^\circ$  and a measuring time of 200 seconds/step.

#### **2.2.6. Transmission electron microscopy**

The morphology of E1NPs was evaluated by transmission electron microscopy (TEM). The E1NPs collected by centrifuging were diluted in Milli-Q water, and 10  $\mu\text{l}$  of the sample (E1NPs) were placed onto the copper EM grids and stained with a 2% (w/v) uranyl acetate solution. After 1 minute, the sample was washed with ultra-purified water and the excess removed using a filter paper. The sample was dried and analyzed.

#### **2.2.7. *In vitro* release studies**

To estimate the profile of E1 release from the NPs, Franz diffusion cells (FDC-400) with a diameter of 18 mm were used. E1-loaded NPs or non-formulated E1 (1 ml) were placed in the donor compartment. The receptor compartment was filled with 5 ml of the receptor medium (1 M phosphate buffer, pH 7.4) and a dialysis cellulose membrane was placed between the donor and receptor compartments of the Franz cells. Sink conditions were maintained throughout the experiment for 24 hours. At predetermined time points, 100- $\mu\text{l}$  aliquots were withdrawn for E1 determination and replaced with fresh medium. A successfully validated HPLC-ESI-MS/MS method was used to determine the amount of E1 released. The concentration of E1 released was measured as previously described in section 2.4. Results are presented as the mean  $\pm$  SD of three replicates. The detection methods were validated following the ICH guidelines<sup>39</sup>. The parameters studied and the results obtained, are summarized in supplementary materials section.

To determine the mechanism of drug release, three different kinetic models (First order, Higuchi and Korsmeyer-peppas) were used to fit the experimental data obtained in the E1 release experiments <sup>40</sup>

$$\text{First order kinetics: } Q_t = Q_\infty(1 - e^{-kt}) \quad (4)$$

$$\text{Higuchi: } Q_t = K_H t^{\frac{1}{2}} \quad (5)$$

$$\text{Peppas-Korsmeyer: } Q_t = K_k t^n \quad (6)$$

Where:

$Q_t$  is the cumulative amount of peptide release at time t; t is time in hours,  $K_H$  Higuchi constant, K is the first-order release constant,  $K_k$  is kinetic constant and n is the diffusional or release exponent, that could be used to characterize the different release mechanism  $n < 0.43$  (Fickian diffusion),  $0.43 < n < 0.85$  (anomalous transport) and  $n \geq 0.85$  (case II transport; i.e. zero-order release).

### 2.2.8. Stability assays

A technology based on the analysis of multiple dispersions of light was used to predict the short-term physical stability of the developed formulations. Turbiscan Lab® (Formulation, L'Union, France) is an optical instrument that characterises concentrated emulsions and dispersions, detecting destabilisation phenomena much earlier than the operator's naked eye, especially for concentrated and optically thick media. One of the principal advantages of using Turbiscan Lab® in the physical stability of the NPs is that the instrument is well suited for working without dilution at high concentrations (up to 95 % v:v), and over a wide particle size range: 10 nm - 1 mm.<sup>41</sup>

Two undiluted formulations were mixed and placed on a cylindrical glass cell, which was scanned by a reading head. The scan was achieved with a pulsed near-infrared light source ( $\lambda = 880$  nm) and two synchronous optical detectors. The transmission (T) detector receives the light transmitted through the sample ( $0^\circ$  from the incident radiation), while the backscattering (BS)

detector receives the light backscattered by the sample ( $135^\circ$  from the incident radiation)<sup>41</sup>. The formulation was milky and opaque; therefore, only BS profiles were used to evaluate the physicochemical stability of E1NPs. The reading head gathered the BS data every  $40\ \mu\text{m}$  for 24 hours. These measurements were performed on samples stored for up to 7 days at  $4\ ^\circ\text{C}$ . These parameters are represented by a curve showing the percentage of BS as a function of the sample height in millimeters. The acquisitions were repeated, generating a superimposition of sample fingerprints that then demonstrated the stability or instability of the sample.

#### **2.2.9. Stability of E1 and E1NPs in human serum**

A suspension of E1-NPs in Hanks Balanced Salt Solution (HBSS) at a peptide concentration of approximately  $1\text{mg/ml}$  was incubated at  $37\ ^\circ\text{C}$  in the presence of 90 % human serum for 24 h. At different incubation times (30 min, 1 h, 2 h, 4 h, 8 h and 24 h),  $50\ \mu\text{l}$  aliquots were treated with  $200\ \mu\text{l}$  of methanol to precipitate serum proteins. After 30 min of centrifugation at 14000 rpm at  $4\ ^\circ\text{C}$  in a centrifuge Mikro 200R Hettich (DJB Labcare Ltd, Buckinghamshire, UK), the supernatant was analysed by RP-HPLC to calculate the percentage of intact peptide in the sample. The analysis of the peptides was carried out on a 1260 Infinity chromatograph (Agilent Technologies, Santa Clara, CA, USA) with a Poroshell 120 EC-C8 (Agilent,  $2.7\ \mu\text{m}$ ,  $4.6\times 100\ \text{mm}$ ). An isocratic method of 55 % of water with 0.05% TFA and 45 % of acetonitrile with 0.05 % TFA was used for analysing the samples.

#### **2.2.10. Uptake assays**

For the uptake assays, NPs were prepared with  $125\ \mu\text{g}$  of E1-FAM. Studies were performed using endothelial cells (HeLa-env donated by Dr Blanco from the Fundació IRSI) that expressed high levels of the Gag, Env, Tat, Rev and Nef proteins and also included the HIV long terminal repeat (LTR) promoter in the genome. The uptake measurements were carried out using the protocol described by Ibuki et al<sup>42,43</sup>. Briefly, HeLa-env cells were seeded onto 6-well plates at  $2\cdot 10^5$  cells/well and incubated under cell culture conditions for 24 hours in Dulbecco's modified

Eagle's medium (DMEM) containing 10% fetal bovine serum (FBS). The cells were then rinsed with phosphate-buffered saline (PBS), and replenished with 1 ml of FBS-free DMEM, containing either empty NPs or E1-FAM-NPs at a concentration of 36  $\mu\text{M}$ , and incubated for predetermined time periods (1, 2, 4, 6 and 24 hours) at 37 °C in 5% CO<sub>2</sub>. Next, the cells were detached from the dishes and washed gently with PBS at least three times to remove the NPs that had not been taken up. Single-cell suspensions for flow cytometry (FCM) were then prepared by the addition of 100  $\mu\text{l}$  of trypsin/EDTA-PBS. Data acquisition was performed using the InCite™ software, where 10,000 events were recorded in the gated regions of interest assigned to the HeLa-env cells.

To discriminate between attached and internalised E1-FAM-NPs, assays measuring 5(6)-FAM quenching by trypan blue were undertaken. 5(6)-FAM signal quenching occurs when trypan blue absorbs the light emitted by E1-FAM-NPs after excitation<sup>44,45</sup>. The 5(6)-FAM signal of internalised E1-FAM-NPs is not quenched since trypan blue cannot pass the plasma membrane. Thus, the fluorescence remaining after trypan blue quenching is from the internalised E1-FAM-NPs since only the extracellular fluorescence of E1-FAM-NPs is quenched.

#### **2.2.11. Mucoadhesive potential of Nanoparticles**

In order to evaluate the mucoadhesive potential of E1NPs and Empty-NPs (GCNPs) a simulated fluid vaginal (SVF) was used, which had previously been developed and described by Owen and Katz<sup>46</sup>. It contained sodium chloride (0.351 %), potassium hydroxide (0.14 %), calcium hydroxide (0.022 %), bovine serum albumin (0.0018 %), lactic acid (0.2 %), acetic acid (0.1 %), glycerol (0.016 %), urea (0.04 %), glucose (0.5 %). Mucin was added at a final concentration of 1.5 %(w/v) and mixed by sonication and vortexing.

The experiments were performed following the protocol described by das Neves et al<sup>16</sup>. The Z-Ave changes of NPs were evaluated using a NPs suspension at a final concentration of 0.2 % v/v added in SVF without mucine (SVF/M-) and SVF with mucine (SVF/M+) (pH 4.2 and pH 7.0). The pH was adjusted by adding minimum amount of hydrochloric acid or sodium

hydroxide. Samples were mixed by vortexing and left to equilibrate for 2 hours at 37 °C before being measured for Z-Ave using a ZetaSizer Nano ZS. The GCNPs utilized presented a Z-Ave of  $273 \pm 1.7$  nm, PI value of  $0.18 \pm 0.01$  and  $\zeta$  of  $19.8 \pm 0.5$  mV.

#### 2.2.12. *Ex vivo* studies

The permeation assays of E1NPs were carried out using the vaginal mucosae of swine, obtained from the animal house at Bellvitge (University of Barcelona). This was done in accordance with the protocol approved by the Ethics Committee of the University of Barcelona<sup>47</sup>.

Permeation studies were carried out following the protocol described in Ariza-Sáenz et al.,<sup>37</sup>. A mixture of receptor medium and Transcutol P® (80:20, v/v) was placed in the receptor compartment, each assay was performed in triplicate.

To determine the permeated amount of E1 at specific time intervals over a period of 6 hours, 300- $\mu$ l aliquots were taken from the receptor chamber and immediately replaced with an equal volume of receptor medium. The apparent permeability coefficient ( $P_{app}$ , cm $\cdot$ s<sup>-1</sup>) of the mucosa was determined using the following equation:

$$P_{app} = \left( \frac{\Delta Q}{\Delta t} \right) \cdot \frac{1}{A \cdot C_0 \cdot 60} \quad (7)$$

where Q is the total amount permeated at time t,  $\Delta Q/\Delta t$  is the steady-step slope of the linear portion of the plot for the amount of peptide in the receptor compartment, A is the exposed diffusion area and  $C_0$  is the initial concentration of peptide.

Statistical comparisons between the samples were performed using one-way ANOVA and the Kruskal-Wallis test. Differences were considered significant at  $p < 0.05$ .

To estimate the amount of E1 retained in the mucosa, a mixture of 1M PBS, pH 7.4, and acetonitrile (80:20, v/v) was used. The mucosal sample was then subjected to 20 minutes of cold sonication in an ultrasound bath. The amount of E1 retained was calculated taking into account

the recovery percentage (R). To determine R, a mucosal slice (non-treated) was weighed and incubated with a solution containing 100  $\mu\text{g/ml}$  of E1 for 6 hours at 37 °C. Both the amount of peptide remaining in solution and the mucosal weight were determined again at the end of the assay. R was calculated with the following equation:

$$R = \frac{\frac{C_p}{m_2}}{\frac{C_1 - C_2}{m_1}} \quad (8)$$

where  $C_p$  is the amount ( $\mu\text{g}$ ) of peptide extracted from the mucosa per 1 ml,  $m_2$  the mucosal slice weight at the end of the assay,  $m_1$  the mucosal slice weight at the beginning of the assay,  $C_1$  the initial E1 concentration (100  $\mu\text{g/ml}$ ) and  $C_2$  the E1 concentration obtained from the solution at the end of the assay. Results were the average of the three independent experiments.

The E1 was quantified by HPLC/MS-MS, and it was expressed as  $\mu\text{g} / (\text{g} \cdot \text{cm}^2)$ . The E1 retained amount was calculated by the equation 9<sup>43</sup>.

$$Q_r = \left( \frac{Ex_x}{Px} \right) / 2.54 \cdot \frac{100}{R} \quad (9)$$

where,  $Q_r$  is the E1 amount retained after the permeation assay through an area of 2.54  $\text{cm}^2$ .  $Ex_x$  is the E1 amount extracted.  $Px$  is the weight of each tissue sample.

### 2.2.13. *In vivo* studies

To determine the amount of E1 retained in the vaginal mucosa, experiments were conducted using four female swine weighing 25 kg each. Before carrying out the experiments, the animals were anaesthetized, and 1 ml aliquots of E1NPs or non-formulated E1 (0.425  $\text{mg/ml}$ ) were applied to the vaginal area. Non-formulated E1 was solubilised with 0.1% DMSO. After 4 hours of incubation, the animals were euthanized, and the intact vaginal mucosa was isolated by

excision with surgical scissors. The tissues were cut into slices of approximately 1 cm<sup>2</sup>. The extraction and quantification of the peptide were carried out as described above.

### 3. RESULTS AND DISCUSSION

#### 3.1. Peptide synthesis

E1 is an 18-mer peptide [WILEYLWKVPDFWVRGVI] with a MW of 2367 Da. It has amphipathic properties and shows significant HIV-1 inhibitory activity through binding to a highly conserved region on gp41 (the fusion peptide), which is essential for viral fusion to target cells<sup>9</sup>. Thus, this peptide could be considered a putative microbicide because it may interact directly with HIV-1. It has been successfully synthesized, achieving a high degree of purity (> 95%) after semi-preparative HPLC purification. The identity of E1 was confirmed by electrospray ionization mass spectrometry (ES-MS) in positive electro spray ionization (ESI) mode. Figure S1 (*supplementary materials section*), shows the mass spectrum of E1 with the most abundant ion at  $m/z$  789.7 ( $z = 3$ ). After E1 fragmentation, several transitions of different molecular weight were obtained and the product ion was at  $m/z$  1189 ( $z = 2$ ). In addition, the identity of E1 and E1-FAM was confirmed by MALDI-TOF spectrometry, and the E1 and E1-FAM spectra are shown in Figures S2a and S2b (*supplementary materials section*), respectively.

#### 3.2. Optimization of E1NPs

The efficacy of drug delivery systems depends on their capacity to release a suitable drug concentration at the site of action. Consequently, we sought to achieve a high peptide entrapment rate. According to the results (*Table S8 in supplementary material section*), the lowest EE value was 13% and the highest was 86.4%, corresponding to F4 (factorial point).

The encapsulation efficiency of E1P47 in nanoparticles was significantly influenced by all the three experimental factors investigated: peptide concentration (A), IAP volume (B) and polymer concentration (C). The response surface analysis of the obtained values led to the following

polynomial regression equation, which quantified the relationship between each of the significant parameters studied and the encapsulation efficiency:

$$\begin{aligned} \text{EE (\%)}: & -1183.0 + 2642.9 (X_1) + 2756.2(X_2) + 546.9(X_3) - 4834.0(X_1)^2 - 1694.6 (X_2)^2 - 321.1 (X_3)^2 \\ & - 2437.2 (X_1) (X_2) + 1286.0 (X_1)(X_3) - 580.1 (X_2)(X_3) \end{aligned} \quad (10)$$

The Z-Ave and PI, which ranged from 176.0 to 443.8 nm and PI, which ranged from 0.06 to 0.41, were mainly influenced by polymer concentration. Increasing the polymer concentration caused the Z-Ave and PI increase, while elevating the IAP volume led to smaller mean nanoparticles size and a decrease in the PI of nanoparticles.

The analysis of the experimental scattering revealed a good reproducibility and proved the reliability of the double emulsion method: (Z-Ave  $265.5 \pm 1.8$  nm and PI:  $0.139 \pm 0.04$ ) (mean  $\pm$  SD, n=3). The polynomial equations are given below (they quantify the relationship between Z-Ave, the PI factor and the parameters studied):

$$\begin{aligned} \text{PI}: & 0.2 + 1.7 (X_1) + 1.1(X_2) - 1.6(X_3) - 6.4(X_1)^2 - 1.1 (X_2)^2 - 1.04(X_3)^2 + 1.03(X_1) (X_2) + 1.4(X_1) \\ & (X_3) - 0.4 (X_2) (X_3) \end{aligned} \quad (11)$$

$$\begin{aligned} \text{Z-Ave (nm)}: & -352.9 + 3477.0 (X_1) + 2025.1(X_2) - 893.8(X_3) - 6857.2(X_1)^2 - 1905.2(X_2)^2 + \\ & 666.3(X_3)^2 - 382.5(X_1) (X_2) + 88.3(X_1) (X_3) - 108.5 (X_2) (X_3). \end{aligned} \quad (12)$$

The response surface plots of factors influencing the EE are represented in Figures 1a and 1b. Likewise, statistical analyses were performed to identify the effect of the factors on Z-Ave, EE and PI. (*Table S9 shows the p values obtained from an ANOVA analysis in the Supplementary Material section*).

Chitosan has attracted a lot of attention as a biomedical material for in addition to the advantages described throughout this manuscript; this biopolymer has immune-stimulating biological, anti-tumor and anti-microbial activities, among others. However, the pharmaceutical applications related to Chitosan are limited by the compound's insolubility at neutral or high pH

values <sup>48</sup>. With the aim of overcoming the insolubility problems associated with a natural polymer, GC was used. This is chitosan (a natural polysaccharide composed of D-glucosamine and N-acetyl D-glucosamine units) conjugated with ethylene glycol. GC is water soluble at a pH below 7.0 and retains its positive charge at physiological pH values <sup>49</sup>.

Therefore, the presence of GC increases NP mucoadhesiveness and retention times at the target site, and endows NPs with a positive surface charge. In addition, GC improves peptide transport across the epithelial barrier <sup>50</sup>.

Table 1. Physicochemical properties and EE of E1NPs and E1FAM-NPs

Formulation	Z-Ave (nm) $\pm$ SD	PI $\pm$ SD	$\zeta$ (mV) $\pm$ SD	EE (%)
E1-NPs	265.5 $\pm$ 1.8 <sup>(a)</sup>	0.1 $\pm$ 0.04 <sup>(a)</sup>	28.0 $\pm$ 0.5	84.6 <sup>(a)</sup>
E1FAM-NPs	316.3 $\pm$ 46.8	0.2 $\pm$ 0.02	32.3 $\pm$ 2.9	60.2

(a) Values obtained from factorial design. Z-Ave, PI and  $\zeta$  values are average of three independent batches, and are expressed as mean  $\pm$  SD.

Although all three factors selected did affect the EE rates, the IAP volume and peptide concentration were the most critical factors ( $p > 0.05$ ). The center values for IAP and peptide concentration were established as 0.5 ml and 1.5 mg/ml, respectively. While these values were maintained, EE rates were higher than 80 %. However, when the peptide concentration fell below the center value and the IAP volume rose above it, the EE rate decreased.

Furthermore, with the objective of increasing the E1 encapsulation rate and decreasing the burst effect on the release, we studied the pH effect on the encapsulation efficiency. First, we studied the effect on the pH using values below the isoelectric point (PI) of the peptide (6.1), and we found that the encapsulation rate was not greater than 5.0 %, and therefore, we decided to use pH higher than this, thereby changing the charge distribution in the peptide and having a positive impact on the encapsulation. We also investigated the inner aqueous phase, as this might affect the peptide's distribution between the inner and outer aqueous phase present in the double emulsion preparation.

In previous studies we were able to determine the influence of the composition of the EE rates. The results obtained from these studies showed that a salt concentration above 50 % gave a higher encapsulation (EE) rate (around 80%). We put this rate down to the dehydration of the emulsifier molecules absorbed on the interface. This led to an increase in inner aqueous droplet size and thickening of the oil membrane <sup>51</sup>. These effects may inhibit membrane rupture and increase the EE rate. Conversely, at a low salt concentration, the oil membrane became thinner and immediate rupture led to a loss of content.

In the light of these findings, E1 was then dissolved in 50 % ACN/50mM Hepes (pH 7.4). The results showed that improvements had been achieved when there had been an accompanying increase in the volume of inner emulsion (a volume of 200 a 500  $\mu$ l).

The efficiency of the encapsulation of a peptide is highly dependent on the method used to prepare the NPs. The selection of a method that gives adequate drug encapsulation depends on the hydrophilicity of the active molecules. Many advantages are associated with the use of the double emulsion method, from which the systems obtained are versatile with respect to the different emulsifiers being employed. With the double emulsion, it is possible to prepare polymeric NPs, which allow the controlled release of the active soluble agent in the internal aqueous phase. Double emulsion is considered as an internal reservoir of trapped active (biomolecule) ingredients in an interior confined space, which protects the peptide from light, enzymatic degradation and oxidation. As for the disadvantages of double emulsion, it is a complex process and thermodynamically unstable. However, it is the unique chemical method which has the advantage of encapsulating both types of molecules, lipophilic and hydrophilic <sup>52</sup>

In order to overcome the disadvantages associated with traditional chemical methods, some authors approached this question with interesting new methods, such as electrohydrodynamic atomization (EHD)<sup>53</sup>, characterized by their simplicity, scalability and high versatility in the tailoring of the surface. Their multifunctionality enables the production of novel and functional materials. With regards to this, recently Parhizkar et al <sup>54</sup> described the fabrication of cisplatin-loaded particles. These obtained high encapsulation rates, controlled release and the safety of the

pharmaceutical compound. This method might be considered as a promising tool for the encapsulation of antiretroviral agents and HIV-inhibitors in chitosan NPs, with nanosized particles with different and adjustable diameters <sup>55</sup>.

### 3.3. Validation of optimized factors

The results of the optimized dependent variables, such as Z-Ave (nm), PI and EE (%) were validated comparing them to the predicted results and what was actually observed. The differences between the predicted and the observed results were found to be from around 5 % and up to 9 % (one significant figure accuracy), as are shown in the table 1. The equation used to calculate the percentage residual value was:

$$\text{Percent residual} = \frac{\text{Predicted results} - \text{Observed results}}{\text{Predicted results}} \times 100 \quad (11)$$

The desirability of the optimized factor (EE) is shown in the chart. Usually, the desirability values fall within the range of 0 to 1, which means nearer the value is to zero (0), the less reliable it is. Whereas, the nearer to one (1) the value is, the more reliable the technique is. Our results demonstrate that the desirability reached the maximum value, which indicates the reliability the method.

Table 2. Validation of optimized factors.

Response factor	Predicted results	Observed results	Residual values (%)
EE (%)	0.98	0.93	5.1
Z-average (nm)	0.34	0.32	5.9
PI	0.22	0.20	9.1

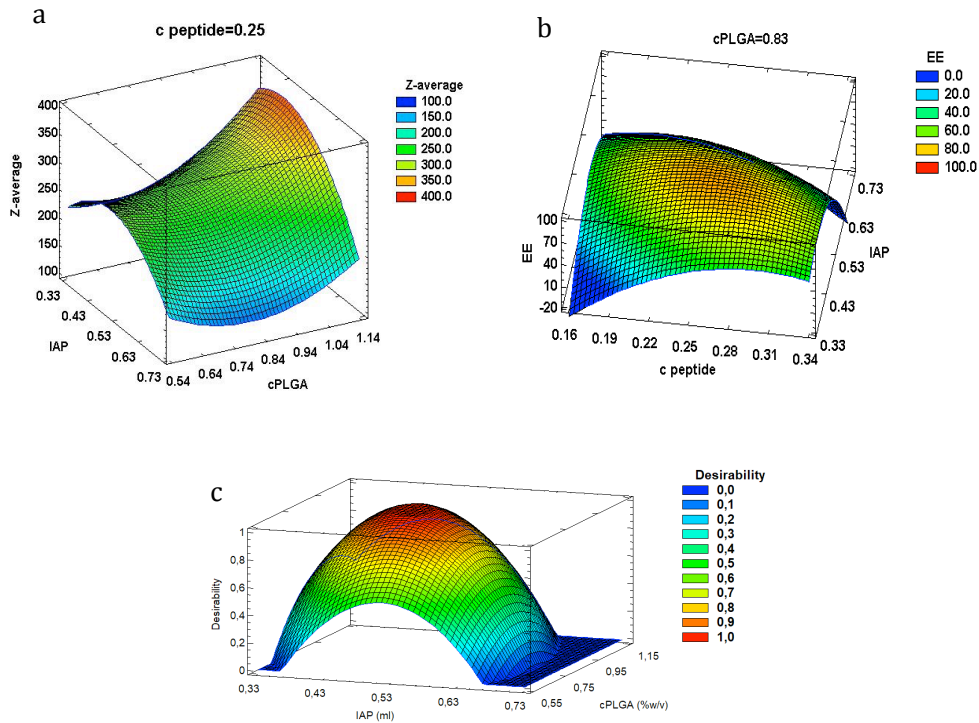


Figure 1. Response surface plots: (a) the effect of IAP and cPLGA on Z-Ave; (b) the effect of IAP and cPeptide on EE; (c) The surface response plot of desirability for optimization of EE factor.

### 3.4. Physicochemical characterization of E1NPs

To determine the physicochemical properties of the NPs, Z-Ave, PI and EE were measured. We also determined the physical status of the peptide inside the NPs and the stability of the suspension.

### 3.5. X-Ray and FTIR studies

By using the x-Ray and FTIR methods we were able to determine the physical state of the E1 trapped in the NPs, as well as the possible interactions with the other components in the formulation.

### 3.5.1. X-Ray

X-Ray shows that PLGA, GC and E1 are of an amorphous nature. However, the X-Ray diffraction of PVA shows a reflection peak at  $2\theta = 19.7^\circ$ , characteristic of crystalline structure. Figure 2 shows X-ray diagrams of E1NPs and their compounds (PLGA, PVA, GC and E1). As can be seen, both the E1 peptide and the E1NPs shared a single weak bulge at  $2\theta = 15.97^\circ$ . Furthermore, an additional bulge was observed at  $2\theta = 19.82^\circ$ , corresponding to GC. The NPs profile was the same as the PLGA, E1 and GC profiles (Figure 2). Together, these observations indicate that the NPs pattern consisted of a combination of two structures. We did not detect the presence of nanocrystals as a consequence of peptide precipitation.

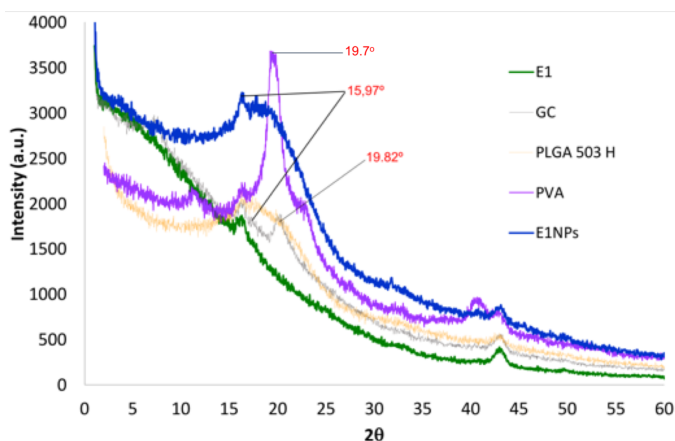


Figure 2. X-ray diagrams: E1NPs and their compounds PLGA, GC, PVA and E1. In addition, to the bulges observed, we can see a prominent peak on the PVA graph, which in distinction to the rest of the compounds shows a crystalline profile.

### 3.5.2. FTIR studies

Figure 3 shows the FTIR spectra of E1, E1NPs and their components. Two prominent bands of the peptide (E1) backbone were present, one corresponding to the amide I band ( $1635.82\text{ cm}^{-1}$ ) and the other to the amide II band ( $1527.35\text{ cm}^{-1}$ ), both of which are shown in the figure. These

bands form the most sensitive spectral region of the secondary structure of proteins and polypeptides <sup>56</sup>. The amide I band (1700-1600  $\text{cm}^{-1}$ ) is mostly due to the C=O stretching vibration of the peptide bond. In the case of amide II, it mainly arises from in-plane NH bending and CN stretching. Amide A (3280  $\text{cm}^{-1}$ ) is the least prominent but it is also related to NH stretching. The presence of bands between 1642 and 1624  $\text{cm}^{-1}$  is assigned to the conformational structure of the  $\beta$ -sheet with contributions from  $\beta$ -turn structures, while the presence of bands between 1654 and 1658  $\text{cm}^{-1}$  is assigned to  $\alpha$ -helix <sup>57</sup>. Therefore, the results indicate that E1 presents a conformational type  $\beta$  structure with contributions from  $\alpha$ -helix. These vibrational bands were repeated in the NPs with less intensity. In addition, E1NPs shared an additional band with PLGA (1762  $\text{cm}^{-1}$ ) due to C-H stretching vibrations in the two polymer monomers <sup>58</sup>. Another observation is that one can see the C-H broad alkyl stretching band ( $n = 2850\text{-}3000 \text{ cm}^{-1}$ ) corresponding to the PVA compound.

These results indicate that E1 has a conformational type  $\beta$  structure, characteristic of medium-sized peptides. The results obtained from a circular dichroism analysis demonstrate that the peptide in the buffer presents a  $\beta$ -type conformation with contributions from  $\beta$ -turn and  $\alpha$ -helix <sup>9</sup>. As one can see (Figure 3), there were no interactions between the components and the peptide.

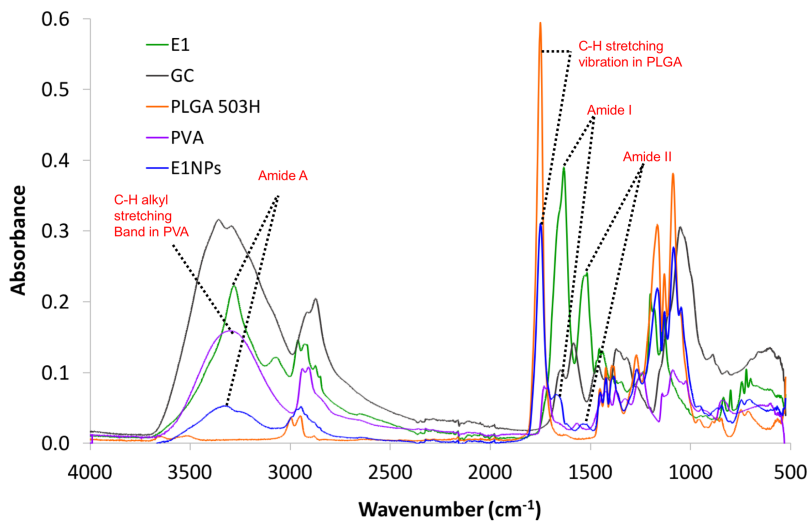


Figure 3. FTIR spectra. This figure shows the FTIR spectra of E1NPs and their compounds: E1, PLGA 503H, PVA and GC.

### 3.6. Transmission electron microscopy analysis

The E1NP images obtained by TEM confirmed the Z-Ave and PI parameters obtained with the factorial design. In addition, the individual non-agglomerated, spherical NPs indicated that the nanoparticles did not aggregate in solution <sup>59</sup>. Figure 4 clearly shows that the E1NPs were spherical with a polymer envelope and an inner cavity.

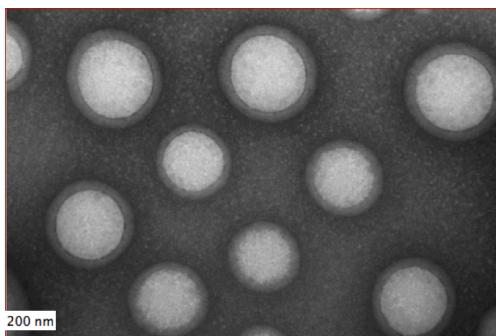


Figure 4. Transmission electron microscopy of E1NPs.

### 3.7. *In vitro* release studies

The E1 release profile is given in Figure 5. At 20 hours the figures show the monophasic release profile of E1, which corresponds to 20 % of the total amount incorporated into the NPs. As E1 is an amphiphilic molecule, it would be erroneous to describe the entire release profile as monophasic, since NPs larger than 200 nm often exhibit a triphasic profile due to heterogeneous degradation<sup>60-62</sup>. Although the E1 was not completely released from the NPs, the mechanism associated with release can be inferred. In general, there are four main release mechanisms: (a) diffusion through water-filled pores, (b) diffusion through the polymer, (c) erosion and (d) osmotic pumping<sup>63</sup>.

Table 3 shows the release constants and release exponents ( $n$ ) calculated by fitting the release data into the respective equations along with regression coefficients ( $R^2$ ). On the basis of  $R^2$  analysis, it could be concluded that the E1NPs followed the Korsmeyer Peppas model (figure 5). Data analysis for E1 released, according to the “Korsmeyer-Peppas” equation indicates the Fickian-diffusion release behaviour ( $n = 0.3$ ;  $R^2 = 0.95$ ) up to 20 hours. These findings can be explained by the swelling of the NPs and this can lead to the creation of fine pores through which the peptide can diffuse outwards.

Table 3. Principal parameters obtained after fitting the release data from the E1NPs to different kinetic model equations

Mathematical Models for E1NPs	Parameters	$R^2$
First order	$K_1 : 0.3$	0.78
Higuchi	$K_H : 0.2$	0.93
Korsmeyer Peppas	$K_1 : 0.4; n : 0.3$	0.95

$K_1$ : first-order constant,  $K_H$ : Higuchi constant,  $K_1$ : Korsmeyer-Peppas constant and  $n$ : diffusional exponent.

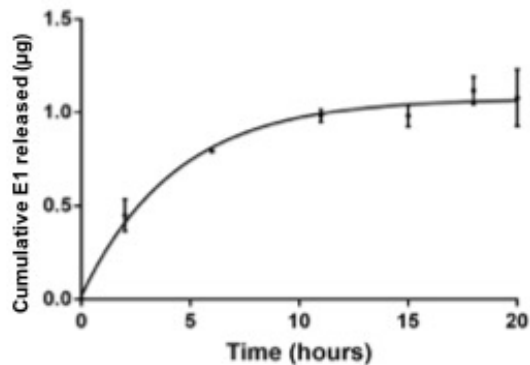


Figure 5. *In vitro* release of E1NPs.

### 3.8. Stability Studies

To determine the phenomena related to the physical destabilisation of the optimized formulation, the suspension was set aside and stored for 7 days at 4°C. Assessment was performed using TurbiscanLab® and measurements were recorded for 24 hours. Variations greater than 10 %, either as a positive or negative value in the graphical scale of backscattering, are representative of an unstable formulation. Figure S3 in supplementary material section gives the backscattering profile of E1NPs. We did not observe any size changes, such as aggregation, coalescence or cremation, associated with physical destabilisation. The backscattering profile was within  $\pm 2\%$ , demonstrating that the formulation was stable under our experimental conditions. The E1NPs suspension may be stable in long-term storage. However, we limited our stability studies to a maximum time so that the NP conditions would be as previously mentioned before in each of the assessments carried out.

### 3.9. Stability of E1 and E1NPs in human serum

One of the main handicaps in the use of peptides in therapy is that they can easily be degraded by proteases, which render them with a short half-life in circulation and gives them poor bioavailability. One common strategy to overcome these obstacles is to protect them by the use of macromolecular carriers such as nanoparticles.

The aim of this assay was to study if the polymeric Nanoparticles (NPs) optimized in this work coated with glycol chitosan and which contain an HIV-1 fusion inhibitor peptide (E1) were able to protect the peptide by making them less accessible to the enzymes in a protease-rich media. To achieve this end, we incubated the free E1 peptide and the E1-NPs separately with human serum. Then aliquots were taken at different points in time. The supernatants were analysed by HPLC. A half-life of approximately 8 hours was obtained for the free E1 peptide. However, an enhanced stability was observed for the peptide entrapped in the NPs, the half-life being increased up to 24 h. In contrast, this improved stability in human serum could be explained by the slow release profile of the peptide from the NPs (figure 5).

### **3.10. Uptake assays**

In order to conduct a flow cytometry analysis, NPs were prepared with E1-FAM, using the composition of the optimized formulation. The differences observed in the Z-Ave, PI,  $\zeta$  and the EE of the E1-FAM-NPs, with respect to the E1-NPs, are attributed to the derivatization of E1 with the fluorescent probes (5(6)-FAM). These differences did not affect the cell studies as the values obtained were within the acceptable range for the studying of cell captures, and therefore it was not necessary to validate them (Table 1).

Cell uptake of NPs is well-documented and has been used to evaluate cytotoxicity, cellular transport mechanisms and intracellular drug delivery<sup>24,64,65</sup>. In this study, cell uptake was assessed to discriminate between the NPs attached to the HeLa-env cell membrane and internalised NPs. HeLa-env cells were treated with E1FAM-NPs at 1, 2, 3, 4, 6 and 24 hours. The results obtained after treatment at 1 to 4 hours showed a time-dependent increase in intensity, while after 6 to 24 hours of treatment, there was a sharp decrease in fluorescence intensity. Thus, in order to discriminate between attached and internalized NPs, HeLa-env cells were treated with E1FAM-NPs and 0.1% TB for 1, 2, 4, 6 and 24 hours. During the first hours, approximately 53% of the NPs were internalised and the remainder (43% to 47%) were attributed to the fluorescence emitted by the NPs attached to the cell membrane (Figure 6a).

Figures 6b and 6c compare HeLa-env cells treated for 4 and 6 hours. At 4 hours, there was an increase in the intensity of side scatter (SS) and forward scatter (FS). However, side scatter and forward scatter intensities decreased over the following hours (6 hours). These two parameters have been used to evaluate both NP internalization and nanotoxicity. The increase in SS intensity represents an increase in granular content within cells due to possible cell uptake or apoptotic body formation. At the same time, the decrease in forward scatter intensity represents a reduction in cell size (they were in fact shrinking). This effect was attributed to constant uptake stimulation, which causes cell death. It has been demonstrated that living cells take up positively charged nanoparticles, disrupting lipid bilayers and eliciting nanoscale defects that enhance conductance through the plasmatic membrane <sup>66</sup>. Once the particle stimulus is removed, cell integrity is recovered, whereas permanent stimulation destabilizes the plasmatic membrane and triggers apoptotic signals leading to cell death <sup>67</sup>.

As for the mechanism of NPs internalization, the surface charge, size and shape of these NPs are the critical factors that determine the cellular fate. It has been reported that polymeric NPs greater in size than 200 nm are easily taken into the cells via clathrin-dependent endocytosis <sup>68</sup>. Other factors associated to the NPs can determine the path of the internalization that leads to the uptake. For example, it has been reported that biopolymers such as chitosan increase the uptake of NPs through endocytosis-mediated receptors <sup>69</sup>.

To date, several reports have discussed the internalization of polymeric nanoparticles into the cells. However, very little has been described on the methods used in the discrimination between NPs adhered to the external membrane and the NPs captured by any of the already well-known mechanisms. Following on along this line, in this study we aimed at determining the percentage of E1NPs that only adhere to the external cellular membrane using the trypan blue stain. We did this bearing in mind that the E1NPs were covered with Glycol Chitosan (GC), and this contributes to the positive superficial charge and strengthens the adherence of the NPs to the epithelial cells <sup>69</sup>. With this straightforward technique one can make a distinction between those E1NPs, which are only “adhered”, and those, which are internalized. This information is core to

this study because the peptide released from the E1NPs adhered to the external membrane could inhibit the fusion of the HIV with the cells.

### **3.11. The mucoadhesive potential of Nanoparticles**

The presence of glycoproteins in the cervical mucus (such as mucine) is the main cause of the electrostatic, hydrophobic and hydrogen bonding interactions with exogenous agents, such as the NPs <sup>70</sup>.

To evaluate the muco-adhesive potential of E1NPs and GCNPs, they were incubated with either SVF/M+ and SVF/M-. Higher increases in the Z-Ave for E1NPs and GCNPs were observed after incubation with SVF/M+. However, the Z-Ave experienced no changes when these were incubated with SVF/M-. These findings may be due to the electrostatic interactions between negative charges of the salicylic acid of mucine and positive charged amine groups of GC that cover the NPs (Figure 7).

We observed that the hydrodynamic changes in GCNPs were higher than in E1NPs. This fact may be due to electrostatic repulsions between mucin and polypeptidic chains that might be adsorbed at the NPs surface.

Likewise, we can observe, the NPs incubated with SVF/M+ at pH 7.0 were slightly larger compared to NPs incubated with SVF/M+ at pH 4.2. These relatively small variations may be attributed to an increase of mucin ionization at pH 7.0, and this in turn may lead to a higher interaction of amine groups of GC.

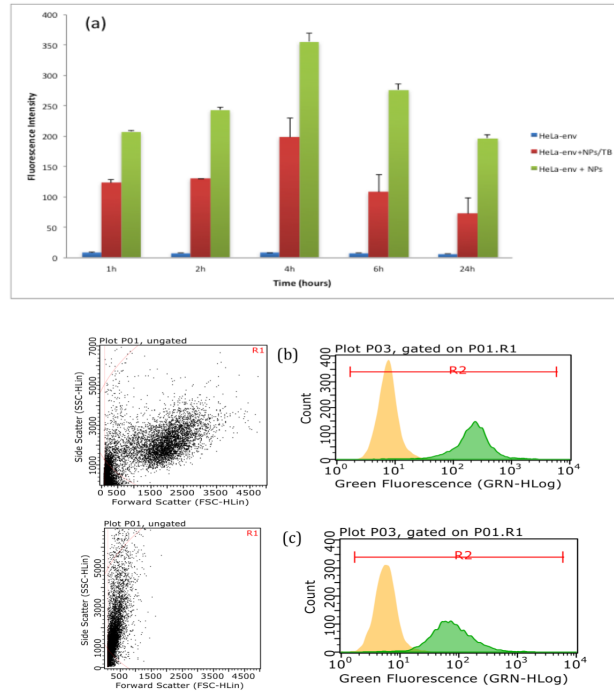


Figure 6. Cell uptake of E1FAM-NPs: (a) cell uptake kinetics of E1FAM-NPs; (b) fluorescence intensity of HeLa-env cells treated for 4 hours with E1FAM-NPs and 0.4% trypan blue dye (TP); (c) fluorescence intensity of HeLa-env cells treated for 6 hours.

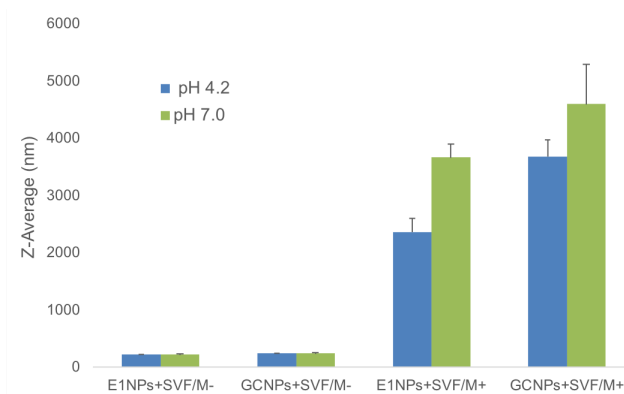


Figure 7. Increase in Z-Average of E1NPs and GCNPs after incubation with SVF with and without mucin at pH 4.0 and 7.0. Columns represent Z-Ave values and the bar standard deviation ( $n=3$ ).

### 3.12. *Ex vivo* and *in vivo* studies

One of the principal preoccupations was to determine the effectiveness of the potential protectiveness and the permeability of the NPs. The swine has been the animal most used to evaluate the permeation through the vaginal mucosa of different types of drugs.

Porcine vaginal mucosa is widely used to evaluate drug permeation for either systemic or local action. Its anatomical, physiological and metabolic characteristics are similar to those of the human vagina, and thus it also has frequently been used to develop microbicides <sup>71</sup>.

However, swine is not a model for studying drug effectiveness as HIV infection does not occur in this animal <sup>72</sup>. This is why in this study we focused on developing a release system that protects against degradation and maintains the HIV inhibitor stability, while at the same time the drug can be released into the vaginal mucosa without causing irritation or any toxicity.

With respect to the evaluation of the effectiveness of the anti-HIV drug, the animals used so far can be classified into small animals and primates. SCID mice have been used and the results have been promising, though like the swine they do not experience natural infection. However, infection in transgenic rabbits has been established, with low levels of viral replication being detected, but only after the animal had been treated with different substances. Infection in chimpanzees and Rhesus monkeys has been limited due to the high costs, the scant availability of these animals and the lack of clinical symptoms. In the case of Rhesus monkeys, research is limited to studies on the HIV envelope and prospective vaccines based on TAT-HIV <sup>73</sup>.

### **3.12.1. *Ex vivo* studies**

The intrinsic mechanisms of NP permeation can be elucidated by *ex vivo* assays <sup>74</sup>. Diffusion mechanisms depend on the physicochemical properties of NPs, the chemical nature of the drug, the lipid/water partition coefficient and the degree of ionization in the molecules permeated through the epithelium.

It has been demonstrated that the permeation of hydrophilic molecules through porcine vaginal mucosa is identical to that through human vaginal mucosa <sup>75</sup>. Drug absorption through the vaginal mucosa occurs via a multi-way mechanism similar to that of biological membranes, and the main

diffusion mechanisms can be passive or active. Passive diffusion includes a transcellular route through the cell membranes, a paracellular route through the intercellular fluid and tight junctions. Active mechanisms generate gradients across the barriers, which are ATP dependent <sup>76</sup>.

The permeation coefficient value calculated for E1NPs and non-formulated E1 (Table 4) showed that the E1NPs were more permeable than non-formulated E1. An ANOVA analysis and the Kruskal-Wallis test revealed significant differences between the  $P_{app}$  obtained for E1NPs and non-formulated E1 ( $p < 0.05$ ).

These results suggest that the physicochemical characteristics of the NPs improved adherence to membranes and diffusion through the mucosa. The fact that there is an 8-fold increase in  $P_{app}$  in the peptide released by NPs may possibly be due to there being no hindrance factor to the penetration - such as a vaginal fluid- which would impede the E1NPs penetrating and going through the mucus. Therefore, the absence of vaginal fluid in the *ex vivo* assays made the penetration of E1NPs through the epithelium easier, and the amount quantified was the result of E1 release of the E1NPs that had penetrated by passive diffusion through the epithelium after 5 hours of experiments. These assays lead to one being able to determine that the surrounding physiologic conditions of the vaginal mucosa, the secretions of fluids, the presence of glycosylated proteins and the bacteria are the main hindrance to the permeation of E1NPs.

Another question is that due to its amphipathic nature, free-E1 could have acquired a secondary structure in cell membranes, which increases their binding. The formation of intramolecular hydrogen bonds in the membrane interface contributes to stronger binding <sup>77</sup>. Thus, the peptide concentration in the upper layer of the mucosa increased, while the E1 permeation rate was decreased.

These findings allow us to conclude that the physiological conditions surrounding the vaginal mucosa, principally the mucine proteins which get tangled up with each other, cause very viscous mucus which prevent the penetration of biomolecules such as E1 <sup>69</sup>.

Table 4.  $P_{app}$  values for E1 permeation of porcine vaginal mucosa after 6 hours.

	$P_{app}$ (cm/s) ( $\pm$ SD)
E1-NPs	$8.9 \times 10^{-3}$ ( $\pm 8.9 \times 10^{-4}$ )
Non-Formulated E1	$1.2 \times 10^{-3}$ ( $\pm 3.2 \times 10^{-4}$ )

Values were calculated as the mean  $\pm$  standard deviation ( $\pm$  S.D).

### 3.12.2. *In vivo* studies

Although in the *ex vivo* studies the conditions to obtain total dissolution of the drug present in the device can easily be established in the laboratory, the biological conditions in which the phenomenon occurs can only be analyzed in the laboratory through *in vivo* studies.

In the case of the transport of macromolecules across the mucosa, this is principally determined by the histophysiological characteristics of the tissue and physiochemical properties of the molecule<sup>78</sup>. With respect to the vaginal fluid, the viscoelastic fluid (mucus) that lines the epithelium, in addition to acting as a protective barrier against pathogens and external agents, can also aid in the access of macromolecules (peptides, proteins, microbicides, etc) to the epithelium. The vaginal mucus is a fluid composed in the greatest part of glycoproteins (mucin), bacteria (lactobacillus) and water<sup>79</sup>.

The results obtained in the *in vivo* studies showed that the E1NPs were capable of interacting with the “mesh mucus” more easily than the non-formulated E1 (Table 5). These phenomena can be explained as a result of the inter-penetrations, which were sufficiently strong, between the polymer and the mucine chains, and which create a semi-permanent adhesiveness that facilitates the crossing of the NPs through the cervical mucus<sup>80</sup>.

The quantity retained (Qr) of formulated E1 that was detected after the treatment of the E1NPs, was significantly greater than the Qr of non-formulated E1 in the mucosa treated only with peptide. This can be put down to the presence of several enzymes in the mucosa, such as lactate dehydrogenase, alkaline phosphates, beta-glucuronidase and esterase. These are the leading causes of the enzymatic degradation of the peptide.

One explanation for the small quantity of non-formulated E1 which did find its way to the vaginal epithelium may be attributed to the fact that non-formulated E1 was solubilised with DMSO, which is considered a permeation enhancer<sup>81</sup>.

The solubility of 100 % of the peptides of an amphiphilic nature requires organic solvents, such as ACN, to be used. In the case of E1 low concentration DMSO was selected to avoid harming the mucosa. It has been reported that in concentrations of DMSO above 60%, protein can be denatured and the intracellular conformation of the keratin can be changed. In the vaginal mucosa, at low concentrations, it is possible that DMSO interacts with the groups at the head of the lipid bilayer so as to distort the geometry of the packaging. This phenomenon can favour the additional partition of the peptide in the DMSO present in the tissue<sup>82</sup>.

From the results obtained from the *in vivo* studies we can conclude that the E1NPs were capable of penetrating the vaginal mucosa, reaching the epithelium and at this point releasing their content, thus protecting against the enzymatic degradation of the peptide.

Together, the *in vivo* and *ex vivo* results highlight the important role of NPs in an effective, safe and protective delivery system for biomolecules such as peptides. They enable the almost impenetrable barrier of the mucosa (due to its lining) to be overcome.

Table 5. *Q* values for E1 released from NPs and non-formulated E1 in *ex vivo* and *in vivo* studies

	<i>Ex vivo</i> ug / (g·cm <sup>2</sup> ) ± (SD)	<i>In vivo</i> µg / (g·cm <sup>2</sup> ) ± (SD)
E1-NPs	38.6 ± 1.6	0.7 ± 0.17
Non-Formulated E1	89.9 ± 2.1	0.4 ± 0.02

Values were calculated as the mean ± standard deviation (± S.D).

#### 4. CONCLUSIONS.

In this paper we have presented a novel strategy to fight the spread of HIV-1 based on polymeric NPs loaded with an HIV-1 fusion inhibitor peptide (E1NPs). The NPs were optimized and characterized to incorporate and release an HIV-1 fusion inhibitor peptide (E1) in porcine vaginal mucosa.

The most important aspects in the development of the NPs, both the modifications made in the method of double emulsion and the selection of the most relevant factors employed in the design and manufacture of the E1NPs, were the over-riding concerns in the development of the NPs so that they had optimum physio-chemical and morphological properties for the encapsulation and release of E1. The results obtained from the analysis of FTIR and X-ray, and the results on physical and chemical stability of the E1 encapsulated in the NPs demonstrate that there were no interactions between the components of the formulation, nor changes in the structure of the E1, nor secondary reactions that could lead to the peptide losing bioactivity.

Our *ex vivo* studies confirmed that NP were able to permeate the vaginal tissue. Despite assay constraints, such as a restricted permeation area, absence of vaginal fluid and an inactive metabolism, we conclude that E1NPs permeate the mucosa more easily than the non-formulated peptide.

From our *in vivo* studies, we are able to conclude that the E1NPs cross the vaginal fluid to reach the epithelium and release the peptide inside. Although a small amount of peptide was extracted from the mucosa treated with non-formulated E1, this finding may be attributed to the presence of DMSO in the solution, which is known to be a permeation enhancer, and therefore does not invalidate our findings.

In addition, we believe that non-formulated E1 might have been partially hydrolysed by enzymes present in the mucus and this is the reason why a small quantity was able to reach the epithelium.

Owing to their physio-chemical, morphological and muco-adhesive properties, and their stability, the E1NPs presented in this study can be considered as a useful platform in the development of an anti-HIV microbicide.

- **Associated content**

Supporting Materials and Methods on the synthesis of E1 and E1-FAM, of analytical methods validation such as HPLC UV-VIS and HPLC MS-MS and additional tables and figures (PDF).

This material is available free of charge via the Internet at <http://>

- **Author information**

Corresponding Author: Ariza-Sáenz Martha

[martharocioariza@gmail.com](mailto:martharocioariza@gmail.com)

[martharocioariza@ub.edu](mailto:martharocioariza@ub.edu)

ORCID: Martha Ariza: 0000-0002-9250-8578

- **Author Contributions**

M.A conceived, designed, and performed the experiments; analysed the data; and wrote the manuscript. I.P.P conducted the cellular assays section and analysed the data A.C. contributed to the conception of *ex vivo* and *in vivo* studies. M.J.G and M.E contributed to and conducted the composite factorial design, and contributed to experimental design and proof-reading of the article. I.H and M.L.G contributed to the conception of the idea, and to the intellectual input and research funding for the study. All authors have given their approval to the final version of the manuscript.

- **Notes**

The authors declare they have no competing financial interests.

## Acknowledgment

The author would like to thank Doctor Joan Blasi, a participant in the study, for his valuable insights throughout the manuscript development. This research was supported by grants from the Spanish Ministry of Economy, Industry and Competitiveness (MINECO) and the European Regional Development Fund (Grants MAT2014-59134-R and CTQ2015-63919-R).

**Abbreviations:** NPs: Nanoparticles; 5 (6)-FAM: 5 (6)- carboxyfluoresceine; E1NPs: Nanoparticles loading fusion inhibitor peptide of HIV-1; E1-FAM: E1 coupled with 5 - (6) carboxyfluoresceine; GC: Glycol-chitosan; HIV-env : Envelope protein of HIV-1.

## REFERENCES

- (1) Schwarze-Zander, C.; Blackard, J. T.; Rockstroh, J. K. Role of GB Virus C in Modulating HIV Disease. *Expert Rev. Anti. Infect. Ther.* **2012**, *10* (5), 563–572.
- (2) Aslan, F. G.; Mustafa, A. Human Pegivirus (GB Virus Type C) and Its Relationship with HIV. *Viral Hepatit J.* **2016**, *22* (3), 113–114.
- (3) Xiang, J.; Wunschmann, S.; Diekema, D. J.; Klinzman, D.; Patrick, K. D.; George, S. L.; Stapleton, J. T. Effect of Coinfection with GB Virus C on Survival among Patients with HIV Infection. *N. Engl. J. Med.* **2001**, *345* (10), 707–714.

- (4) Jung, S.; Knauer, O.; Donhauser, N.; Eichenmüller, M.; Helm, M.; Fleckenstein, B.; Reil, H. Inhibition of HIV Strains by GB Virus C in Cell Culture Can Be Mediated by CD4 and CD8 T-Lymphocyte Derived Soluble Factors. *AIDS* **2005**, *19* (12), 1267–1272.
- (5) Allison, S. L.; Schalich, J.; Stiasny, K.; Mandl, W.; Heinz, F. X. Mutational Evidence for an Internal Fusion Peptide in Flavivirus Envelope Protein E Mutational Evidence for an Internal Fusion Peptide in Flavivirus Envelope Protein E. *J. Virol.* **2001**, *75* (9), 4268–4275.
- (6) Larios, C.; Min, J.; Haro, I.; Alsina, M. A.; Busquets, M. A. Study of Adsorption and Penetration of E2 ( 279-298 ) Peptide into Langmuir Phospholipid Monolayers. *Langmuir* **2006**, *2*, 23292–23299.
- (7) Larios, C.; Casas, J.; Mestres, C.; Haro, I.; Alsina, M. A. Perturbations Induced by Synthetic Peptides from Hepatitis G Virus Structural Proteins in Lipid Model Membranes: A Fluorescent Approach. *Luminescence* **2005**, *20* (4–5), 279–281.
- (8) Pérez-López, S.; Vila-Romeu, N.; Esteller, M. A. A.; Espina, M.; Haro, I.; Mestres, C. Interaction of GB Virus C/Hepatitis G Virus Synthetic Peptides with Lipid Langmuir Monolayers and Large Unilamellar Vesicles. *J. Phys. Chem. B* **2009**, *113* (1), 319–327.
- (9) Gómara, M. J.; Sánchez-Merino, V.; Paús, A.; Merino-Mansilla, A.; Gatell, J. M.; Yuste, E.; Haro, I. Definition of an 18-Mer Synthetic Peptide Derived from the GB Virus C E1 Protein as a New HIV-1 Entry Inhibitor. *Biochim. Biophys. Acta - Gen. Subj.* **2016**, *1860* (6), 1139–1148.
- (10) Sánchez-Martín, M. J.; Hristova, K.; Pujol, M.; Gómara, M. J.; Haro, I.; Asunción Alsina, M.; Antònia Busquets, M. Analysis of HIV-1 Fusion Peptide Inhibition by Synthetic Peptides from E1 Protein of GB Virus C. *J. Colloid Interface Sci.* **2011**, *360* (1), 124–131.

- (11) Münch, J.; Ständker, L.; Adermann, K.; Schulz, A.; Schindler, M.; Chinnadurai, R.; Pöhlmann, S.; Chaipan, C.; Biet, T.; Peters, T.; et al. Discovery and Optimization of a Natural HIV-1 Entry Inhibitor Targeting the Gp41 Fusion Peptide. *Cell* **2007**, *129* (2), 263–275.
- (12) Kilby, J. M.; Hopkins, S.; Venetta, T. M.; DiMassimo, B.; Cloud, G. A.; Lee, J. Y.; Alldredge, L.; Hunter, E.; Lambert, D.; Bolognesi, D.; et al. Potent Suppression of HIV-1 Replication in Humans by T-20, a Peptide Inhibitor of Gp41-Mediated Virus Entry. *Nat. Med.* **1998**, *4* (11), 1302–1307.
- (13) Eissmann, K.; Mueller, S.; Sticht, H.; Jung, S.; Zou, P.; Jiang, S.; Gross, A.; Eichler, J.; Fleckenstein, B.; Reil, H. HIV-1 Fusion Is Blocked through Binding of GB Virus C E2D Peptides to the HIV-1 Gp41 Disulfide Loop. *PLoS One* **2013**, *8* (1), 1–15.
- (14) Vlieghe, P.; Lisowski, V.; Martinez, J.; Khrestchatisky, M. Synthetic Therapeutic Peptides : Science and Market. *Drug Discov. Today* **2010**, *15* (January), 40–56.
- (15) Rohan, L. C.; Sassi, A. B. Vaginal Drug Delivery Systems for HIV Prevention. *AAPS J.* **2009**, *11* (1), 78–87.
- (16) Neves, J.; Rocha, C. M. R.; Gonç, M. P.; Carrier, R. L.; Amiji, M.; Maria, J.; Bahia, F.; Sarmiento, B. Interactions of Microbicide Nanoparticles with a Simulated Vaginal Fluid. *Mol. Pharm.* **2012**, *9*, 3347–3556.
- (17) Brako, F.; Mahalingam, S.; Rami-Abraham, B.; Craig, D. Q. M.; Edirisinghe, M. Application of Nanotechnology for the Development of Microbicides. *Nanotechnology* **2017**, *28* (5), 1–21.
- (18) Meng, J.; Agrahari, V.; Ezoulin, M. J.; Zhang, C.; Purohit, S. S.; Molteni, A.; Dim, D.; Oyler, N. A.; Youan, B. B. C. Tenofovir Containing Thiolated Chitosan Core/Shell Nanofibers: In Vitro and in Vivo Evaluations. *Mol. Pharm.* **2016**, *13* (12), 4129–4140.

- (19) Patel, A.; Patel, M.; Yang, X.; Mitra, A. K.; City, K. Recent Advances in Protein and Peptide Drug Delivery: A Special Emphasis on Polymeric Nanoparticles. *Protein Pept Lett* **2014**, *21* (11), 1102–1120.
- (20) Woodsong, C.; Holt, J. D. S. Acceptability and Preferences for Vaginal Dosage Forms Intended for Prevention of HIV or HIV and Pregnancy. *Adv. Drug Deliv. Rev.* **2015**, *92*, 146–154.
- (21) Mohanraj, V.; Chen, Y.; Chen, M. &. Nanoparticles – A Review. *Trop. J. Pharm. Res.* *Trop J Pharm Res* **2006**, *5* (June), 561–573.
- (22) Salem, S. A.; Hwei, N. M.; Saim, A. Bin; Ho, C. C. K.; Sagap, I.; Singh, R.; Yusof, M. R.; Md Zainuddin, Z.; Bt. Hj Idrus, R. Polylactic-Co-Glycolic Acid Mesh Coated with Fibrin or Collagen and Biological Adhesive Substance as a Prefabricated, Degradable, Biocompatible, and Functional Scaffold for Regeneration of the Urinary Bladder Wall. *J. Biomed. Mater. Res. - Part A* **2013**, *101 A* (8), 2237–2247.
- (23) Makadia, H. K.; Steven J Siegel. Poly Lactic-Co-Glycolic Acid (PLGA) as Biodegradable Controlled Drug Delivery Carrier. *J. Polym. Sci. Part B Polym. Phys.* **2011**, *3* (3), 1377–1397.
- (24) Nkabinde, L. A.; Shoba-Zikhali, L. N. N.; Semete-Makokotlela, B.; Kalombo, L.; Swai, H.; Grobler, A.; Hamman, J. H. Poly (D,L-Lactide-Co-Glycolide) Nanoparticles: Uptake by Epithelial Cells and Cytotoxicity. *Express Polym. Lett.* **2014**, *8* (3), 197–206.
- (25) Anderson, J. M.; Shive, M. S. Biodegradation and Biocompatibility of PLA and PLGA Microspheres. *Adv. Drug Deliv. Rev.* **2012**, *64* (SUPPL.), 72–82.
- (26) Bonferoni, M. C.; Sandri, G.; Rossi, S.; Ferrari, F.; Gibin, S.; Caramella, C. Chitosan Citrate as Multifunctional Polymer for Vaginal Delivery. Evaluation of Penetration Enhancement and Peptidase Inhibition Properties. *Eur. J. Pharm. Sci.* **2008**, *33* (2), 166–176.

- (27) Tao, Y.; Zhang, H. L.; Hu, Y. M.; Wan, S.; Su, Z. Q. Preparation of Chitosan and Water-Soluble Chitosan Microspheres via Spray-Drying Method to Lower Blood Lipids in Rats Fed with High-Fat Diets. *Int. J. Mol. Sci.* **2013**, *14* (2), 4174–4184.
- (28) Takeuchi, H.; Yamamoto, H.; Kawashima, Y. Mucoadhesive Nanoparticulate Systems for Peptide Drug Delivery. *Adv. Drug Deliv. Rev.* **2001**, *47* (1), 39–54.
- (29) Meng, J.; Sturgis, T. F.; Youan, B. B. C. Engineering Tenofovir Loaded Chitosan Nanoparticles to Maximize Microbicide Mucoadhesion. *Eur. J. Pharm. Sci.* **2011**, *44* (1–2), 57–67.
- (30) Frank, L. A.; Sandri, G.; D’Autilia, F.; Contri, R. V.; Bonferoni, M. C.; Caramella, C.; Frank, A. G.; Pohlmann, A. R.; Guterres, S. S. Chitosan Gel Containing Polymeric Nanocapsules: A New Formulation for Vaginal Drug Delivery. *Int. J. Nanomedicine* **2014**, *9* (1), 3151–3161.
- (31) Haggag, Y. A.; Faheem, A. M. Evaluation of Nano Spray Drying as a Method for Drying and Formulation of Therapeutic Peptides and Proteins. *Front. Pharmacol.* **2015**, *6* (July), 1–5.
- (32) Anthony S. Ham; Cost, M. R.; Sassi, A. B.; Dezzutti, C. S.; Rohan1, L. C. Targeted Delivery of PSC-RANTES for HIV-1 Prevention Using Biodegradable Nanoparticles. *Pharm. Res.* **2014**, *26* (3), 502–511.
- (33) Klatt, N. R.; Cheu, R.; Birse, K.; Zevin, A. S.; Perner, M.; Noël-romas, L.; Grobler, A.; Westmacott, G.; Xie, I. Y.; Butler, J.; et al. Vaginal Bacteria Modify HIV Tenofovir Microbicide Efficacy in Africanwomen. *Science (80-. )*. **2017**, *356* (June), 938–945.
- (34) Meng, F. T.; Ma, G. H.; Qiu, W.; Su, Z. G. W/O/W Double Emulsion Technique Using Ethyl Acetate as Organic Solvent: Effects of Its Diffusion Rate on the Characteristics of Microparticles. *J. Control. Release* **2003**, *91* (3), 407–416.

- (35) Silva, A. L.; Rosalia, R. A.; Sazak, A.; Carstens, M. G.; Ossendorp, F.; Oostendorp, J.; Jiskoot, W. Optimization of Encapsulation of a Synthetic Long Peptide in PLGA Nanoparticles: Low-Burst Release Is Crucial for Efficient CD8+ T Cell Activation. *Eur. J. Pharm. Biopharm.* **2013**, *83* (3), 338–345.
- (36) Agnihotri, S. M.; Vavia, P. R. Influences of Process Parameters on Nanoparticle Preparation Performed by a Double Emulsion Ultrasonication Technique. *J. Surf. Sci. Technol.* **2003**, *19* (3–4), 183–187.
- (37) Ariza-sáenz, M.; Espina, M.; Bolaños, N.; Cristina, A.; José, M.; Haro, I.; Luisa, M. Penetration of Polymeric Nanoparticles Loaded with an HIV-1 Inhibitor Peptide Derived from GB Virus C in a Vaginal Mucosa Model. *Eur. J. Pharm. Biopharm.* **2017**, *120* (August), 98–106.
- (38) Leardi, R. Experimental Design in Chemistry: A Tutorial. *Anal. Chim. Acta* **2009**, *652* (1–2), 161–172.
- (39) International Conference on Harmonisation. *ICH Harmonised Tripartite Guideline. Validation of Analytical Procedures: Text and Methodology Q2 (R1)*; 2005; pp 1–13.
- (40) Abrego, G.; Alvarado, H.; Souto, E. B.; Guevara, B.; Bellowa, L. H.; Parra, A.; Calpena, A.; Garcia, M. L. Biopharmaceutical Profile of Pranoprofen-Loaded PLGA Nanoparticles Containing Hydrogels for Ocular Administration. *Eur. J. Pharm. Biopharm.* **2015**, *95* (February), 261–270.
- (41) Mengual, O.; Meunier, G.; Cayré, I.; Puech, K.; Snabre, P. TURBISCAN MA 2000: Multiple Light Scattering Measurement for Concentrated Emulsion and Suspension Instability Analysis. *Talanta* **1999**, *50* (2), 445–456.

- (42) Suzuki, H.; Toyooka, T.; Ibuki, Y. Simple and Easy Method to Evaluate Uptake Potential of Nanoparticles in Mammalian Cells Using a Flow Cytometric Light Scatter Analysis. *Environ. Sci. Technol* **2007**, *41* (8), 3018–3024.
- (43) Ibuki, Y.; Toyooka, T. Nanoparticle Uptake Measured by Flow Cytometry. In *Nanotoxicity: Methods and protocols, Methods in Molecular Biology*; Joshua Reineke, Ed.; 2012; Vol. 926, pp 157–166.
- (44) Vranic, S.; Boggetto, N.; Contremoulins, V.; Mornet, S.; Reinhardt, N.; Marano, F.; Baeza-Squiban, A.; Boland, S. Deciphering the Mechanisms of Cellular Uptake of Engineered Nanoparticles by Accurate Evaluation of Internalization Using Imaging Flow Cytometry. *Part. Fibre Toxicol.* **2013**, *10* (2), 1–16.
- (45) Simons, E. R. Measurement of Phagocytosis and of the Phagosomal Environment in Polymorphonuclear Phagocytes by Flow Cytometry. *Curr Protoc Cytom* **2011**, 1–10.
- (46) Owen, D. H.; Katz, D. F. A Vaginal Fluid Simulant. *Contraception* **1999**, *59* (2), 91–95.
- (47) Muthu, E.; Balakrishnan, P.; Vignesh, R.; Velu, V.; Jayakumar, P.; Solomon, S. Current Views on the Pathophysiology of GB Virus C Coinfection with HIV-1 Infection. *Curr Infect Dis Rep* **2011**, *13*, 47–52.
- (48) Vanden Braber, N. L.; Díaz Vergara, L. I.; Morán Vieyra, F. E.; Borsarelli, C. D.; Yossen, M. M.; Vega, J. R.; Correa, S. G.; Montenegro, M. A. *Physicochemical Characterization of Water-Soluble Chitosan Derivatives with Singlet Oxygen Quenching and Antibacterial Capabilities*; Elsevier B.V., 2017; Vol. 102.
- (49) Trapani, A.; Sitterberg, J.; Bakowsky, U.; Kissel, T. The Potential of Glycol Chitosan Nanoparticles as Carrier for Low Water Soluble Drugs. *Int. J. Pharm.* **2009**, *375* (1–2), 97–106.

(50) Van Der Merwe, S. M.; Verhoef, J. C.; Verheijden, J. H. M.; Kotzé, A. F.; Junginger, H. E. Trimethylated Chitosan as Polymeric Absorption Enhancer for Improved Peroral Delivery of Peptide Drugs. *Eur. J. Pharm. Biopharm.* **2004**, *58* (2), 225–235.

(51) Hino, T.; Shimabayashi, S.; Tanaka, M.; Nakano, M.; Okochi, H. Improvement of Encapsulation Efficiency of Water-in-Oil-in-Water Emulsion with Hypertonic Inner Aqueous Phase. *J. Microencapsul.* **2001**, *18* (November), 19–28.

(52) Teekamp, N.; Duque, L. F.; Frijlink, H. W.; Hinrichs, W. L. J.; Teekamp, N.; Duque, L. F.; Frijlink, H. W.; Hinrichs, W. L. J. Production Methods and Stabilization Strategies for Polymer-Based Nanoparticles and Microparticles for Parenteral Delivery of Peptides and Proteins. *Expert Opin. Drug Deliv.* **2015**, *5247* (August 2017).

(53) Xie, J.; Jiang, J.; Davoodi, P.; Srinivasan, M. P.; Wang, C. H. Electrohydrodynamic Atomization: A Two-Decade Effort to Produce and Process Micro-/Nanoparticulate Materials. *Chem. Eng. Sci.* **2015**, *125*, 32–57.

(54) Parhizkar, M.; Reardon, P. J. T.; Knowles, J. C.; Browning, R. J.; Stride, E.; Barbara, P. R.; Harker, A. H.; Edirisinghe, M. Electrohydrodynamic Encapsulation of Cisplatin in Poly (Lactic-Co-Glycolic Acid) Nanoparticles for Controlled Drug Delivery. *Nanomedicine Nanotechnology, Biol. Med.* **2016**, *12* (7), 1919–1929.

(55) Zhang, S.; Kawakami, K. One-Step Preparation of Chitosan Solid Nanoparticles by Electro spray Deposition. *Int. J. Pharm.* **2010**, *397* (1–2), 211–217.

(56) Kong Shaoning, J. Fourier Transform Infrared Spectroscopic Analysis of Protein Secondary Structures Protein FTIR Data Analysis and Band Assign-. *Acta Biochim. Biophys. Sin. (Shanghai)*. **2007**, *39* (8), 549–559.

(57) Darmon, S. E.; Sutherland, G. B. B. Infrared Spectra and Structure of Natural and Synthetic Polypeptides. *J. Am. Chem. Soc.* **1947**, *979* (1), 2074.

- (58) Jones, A. W.; Cooper, H. J. Dissociation Techniques in Mass Spectrometry-Based Proteomics. *Analyst* **2011**, *136*, 3419–3429.
- (59) Ma, H.; Shieh, K.; Qiao, T. X. Study of Transmission Electron Microscopy ( TEM ) and Scanning Electron Microscopy ( SEM ). *Nat. Sci.* **2006**, *4* (3), 14–22.
- (60) Berkland, C.; King, M.; Cox, A.; Kim, K.; Pack, D. W. Precise Control of PLG Microsphere Size Provides Enhanced Control of Drug Release Rate. *J. Control. Release* **2002**, *82* (1), 137–147.
- (61) Berchane, N. S.; Carson, K. H.; Rice-Ficht, A. C.; Andrews, M. J. Effect of Mean Diameter and Polydispersity of PLG Microspheres on Drug Release: Experiment and Theory. *Int. J. Pharm.* **2007**, *337* (1–2), 118–126.
- (62) Mulye, N. V.; Turco, S. J. A Simple Model Based on First Order Kinetics to Explain Release of Highly Water Soluble Drugs from Porous Dicalcium Phosphate Dihydrate Matrices. *Drug Dev. Ind. Pharm.* **1995**, *21* (8), 943–953.
- (63) Fredenberg, S.; Wahlgren, M.; Reslow, M.; Axelsson, A. The Mechanisms of Drug Release in Poly(Lactic-Co-Glycolic Acid)-Based Drug Delivery Systems--a Review. *Int. J. Pharm.* **2011**, *415* (1–2), 34–52.
- (64) Lai, Y.; Chiang, P. C.; Blom, J. D.; Li, N.; Shevlin, K.; Brayman, T. G.; Hu, Y.; Selbo, J. G.; Hu, L. G. Comparison of in Vitro Nanoparticles Uptake in Various Cell Lines and in Vivo Pulmonary Cellular Transport in Intratracheally Dosed Rat Model. *Nanoscale Res. Lett.* **2008**, *3* (9), 321–329.
- (65) Win, K. Y.; Feng, S. S. Effects of Particle Size and Surface Coating on Cellular Uptake of Polymeric Nanoparticles for Oral Delivery of Anticancer Drugs. *Biomaterials* **2005**, *26* (15), 2713–2722.

(66) Leroueil, P. R.; Berry, S. A.; Duthie, K.; Han, G.; Rotello, V. M.; McNerny, D. Q.; Baker, J. R.; Orr, B. G.; Holl, M. M. B. Wide Varieties of Cationic Nanoparticles Induce Defects in Supported Lipid Bilayers. *Nano Lett.* **2008**, *8* (2), 420–424.

(67) Pina, M. F.; Lau, W.; Scherer, K.; Parhizkar, M.; Edirisinghe, M.; Craig, D. The Generation of Compartmentalized Nanoparticles Containing SiRNA and Cisplatin Using a Multi-Needle Electrohydrodynamic Strategy. *Nanoscale* **2017**, *9* (18), 5975–5985.

(68) Nam, H. Y.; Kwon, S. M.; Chung, H.; Lee, S. Y.; Kwon, S. H.; Jeon, H.; Kim, Y.; Park, J. H.; Kim, J.; Her, S.; et al. Cellular Uptake Mechanism and Intracellular Fate of Hydrophobically Modified Glycol Chitosan Nanoparticles. *J. Control. Release* **2009**, *135* (3), 259–267.

(69) Duceppe, N.; Tabrizian, M. Advances in Using Chitosan-Based Nanoparticles for *in Vitro* and *in Vivo* Drug and Gene Delivery. *Expert Opin. Drug Deliv.* **2010**, *7* (10), 1191–1207.

(70) McGill, S. L.; Smyth, H. D. C. Disruption of the Mucus Barrier by Topically Applied Exogenous Particles. *Mol. Pharm.* **2010**, *7* (6), 2280–2288.

(71) D’Cruz, O. J.; Uckun, F. M. Vaginal Microbicides and Their Delivery Platforms. *Expert Opin. Drug Deliv.* **2014**, *11* (5), 723–740.

(72) Squier, C. A.; Mantz, M. J.; Schlievert, P. M.; Davis, C. C. Porcine Vagina Ex Vivo as a Model for Studying Permeability and Pathogenesis in Mucosa. *J. Pharm. Sci.* **2008**, *97* (1), 9–21.

(73) Hatzioannou, T.; Evans, D. T. Animal Models for HIV/AIDS Research. *Natl. Inst. Heal.* **2012**, *10* (12), 852–867.

(74) Machado, R. M.; Palmeira-de-Oliveira, A.; Gaspar, C.; Martinez-de-Oliveira, J.; Palmeira-de-Oliveira, R. Studies and Methodologies on Vaginal Drug Permeation. *Adv. Drug Deliv. Rev.* **2015**, *92*, 14–26.

(75) Van Eyk, A. D.; Van Der Bijl, P. Comparative Permeability of Various Chemical Markers through Human Vaginal and Buccal Mucosa as Well as Porcine Buccal and Mouth Floor Mucosa. *Arch. Oral Biol.* **2004**, *49* (5), 387–392.

(76) Machado, A.; Neves, J. das. *Tissue-Based in Vitro and Ex Vivo Models for Dermal Permeability Studies*; Elsevier Ltda, 2016.

(77) Mónica Fernández-vidal, Sajith Jayasinghe, Alexey S, L. and S. H. W. Folding Amphipathic Helices into Membranes: Amphiphilicity Trumps Hydrophobicity. *J Mol Biol* **2007**, *370* (3), 459–470.

(78) Machado, R. M.; Palmeira-de-Oliveira, A.; Gaspar, C.; Martinez-de-Oliveira, J.; Palmeira-de-Oliveira, R. Studies and Methodologies on Vaginal Drug Permeation. *Advanced Drug Delivery Reviews*. 2015, pp 14–26.

(79) Ensign, L. M.; Cone, R.; Hanes, J. Nanoparticle-Based Drug Delivery to the Vagina: A Review. *J. Control. Release* **2014**, *190*, 500–514.

(80) Boddupalli, B.; Mohammed, Z. .; Nath, R.; Banji, D. Mucoadhesive Drug Delivery System: An Overview. *J. Adv. Pharm. Technol. Res.* **2010**, *1* (4), 381–387.

(81) Marren, K. Dimethyl Sulfoxide: An Effective Penetration Enhancer for Topical Administration of NSAIDs. *Phys Sport.* **2011**, *39* (3), 75–82.

(82) Takeuchi, H.; Thongborisute, J.; Matsui, Y.; Sugihara, H.; Yamamote, H.; Kawashima, Y. Novel Mucoadhesion Tests for Polymers and Polymer-Coated Particles to Design Optimal Mucoadhesive Drug Delivery Systems. *Adv. Drug Deliv. Rev.* **2005**, *57* (11), 1583–1594.

